Unclassified DTIC FILE COPY
SECURITY CLASSIFICATION OF THIS PAGE

(2)

REPORT DOCUMENTATION PAGE

Form Approved
OMB No. 0704-0188

1a. REPORT SECURITY CLASSIFICATION Unclassified	1b. RESTRICTIVE MARKINGS
2a. SECURITY CLASSIFICATION AUTHORITY	3. DISTRIBUTION/AVAILABILITY OF REPORT Approved for public release; distribution is unlimited
2b. DECLASSIFICATION/DOWNGRADING SCHEDULE	
4. PERFORMING ORGANIZATION REPORT NUMBER(S) AD-A221 005	5. MONITORING ORGANIZATION REPORT NUMBER(S) AFOSR-TR- 90-0514
6a. NAME OF PERFORMING ORGANIZATION University of Colorado	6b. OFFICE SYMBOL (If applicable)
6c. ADDRESS (City, State, and ZIP Code) Dept. of Chemistry & Biochemistry University of Colorado Boulder, CO 80309-0195	7a. NAME OF MONITORING ORGANIZATION AFOSR/NC
	7b. ADDRESS (City, State, and ZIP Code) Building 410 Bolling AFB Washington, DC 20332-6448
8a. NAME OF FUNDING/SPONSORING ORGANIZATION AFOSR	8b. OFFICE SYMBOL (If applicable) NC
8c. ADDRESS (City, State, and ZIP Code) Building 410, Bolling AFB DC 20332-6448	9. PROCUREMENT INSTRUMENT IDENTIFICATION NUMBER F49620-86-C-0056
	10. SOURCE OF FUNDING NUMBERS PROGRAM ELEMENT NO. 61102F; PROJECT NO. 2303; TASK NO B1; WORK UNIT ACCESSION NO.

11. TITLE (Include Security Classification)
IR Transition Moments and Collisional Dynamics of Vibrationally Excited OH Radicals via Time-Resolved Laser Absorption Spectroscopy (Unclassified)

12. PERSONAL AUTHOR(S)
David J. Nesbitt

13a. TYPE OF REPORT	13b. TIME COVERED	14. DATE OF REPORT (Year, Month, Day)	15. PAGE COUNT
final	FROM 1986 TO 1989	1990 March 30	18

16. SUPPLEMENTARY NOTATION

17. COSATI CODES			18. SUBJECT TERMS (Continue on reverse if necessary and identify by block number)
FIELD	GROUP	SUB-GROUP	
			OH radical; flash kinetic spectroscopy; IR laser absorption; dipole moment function

19. ABSTRACT (Continue on reverse if necessary and identify by block number)

A high resolution, IR laser flash kinetic spectrometer has been constructed for time-resolved study of reactive kinetics, energy transfer, and radiative properties of atmospheric OH radicals. Theoretical efforts predict a dramatic J dependence to OH vibrational radiative rates, which are exploited experimentally in the flash kinetic spectrometer to infer an empirical dipole moment function. The accuracy of this dipole moment function is extended to include the turning points of up to OH(v=9) by use of rotationally resolved emission from FTIR studies of the $H + O_3^*$ chemiluminescent reaction. The explicit knowledge of the state-to-state radiative rates permits an absolute measurement of the quantum yields for 193 and 248 nm photolysis production of OH from HNO_3^* and H_2O_2. Reaction rates of OH with atmospheric hydrocarbons are investigated, as well as the relaxation processes of highly rotationally excited OH formed by excimer laser photolysis of HNO_3. This information bears directly on the characterization of highly vibrationally and rotationally excited OH "airglow" emission from the stratosphere.

20. DISTRIBUTION/AVAILABILITY OF ABSTRACT	21. ABSTRACT SECURITY CLASSIFICATION
☒ UNCLASSIFIED/UNLIMITED ☐ SAME AS RPT ☐ DTIC USERS	Unclassified

22a. NAME OF RESPONSIBLE INDIVIDUAL	22b. TELEPHONE (Include Area Code)	22c. OFFICE SYMBOL
F. J. Wodarczyk	(202) 767-4963	AFOSR/NC

DD Form 1473, JUN 86 — Previous editions are obsolete. — SECURITY CLASSIFICATION OF THIS PAGE: Unclassified

90 04 27 049

SUMMARY OF RESEARCH ACCOMPLISHMENTS UNDER AFOSR FUNDING (1986-present)

The focus of the present granting period has been to develop and exploit a high resolution IR laser flash kinetic spectrometer for detailed study of OH radical in the ground electronic state (see Fig. 1). The spectrometer is based on excimer laser photolysis of precursors in a fast flow reactor, followed by time resolved, shot noise limited detection ($<10^{-6}/\sqrt{Hz}$) of the weak OH(Δv=1) absorption signals with a single mode, tunable F-center laser. The significant achievements of the past 3 years on the project with this flash kinetic spectrometer are briefly summarized below.

A. Novel Scheme for F-Center Single Mode Scan Control

In order to utilize the flash kinetic spectrometer in an efficient manner searching for weak absorption signals from transient radicals, it has proven

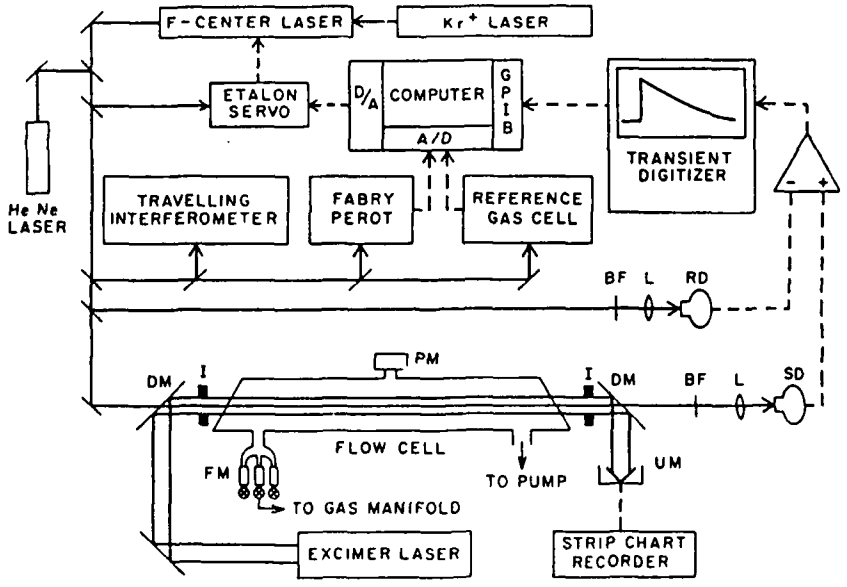

Fig. 1. Schematic of the tunable F-center laser flash kinetic spectrometer apparatus.

quite useful to be able to tune the single frequency laser continuously over $\lesssim 1$ cm^{-1} via a simple external control voltage. We therefore have developed[1] a novel scheme for continuous single frequency scanning of a commercial F-center laser, complementing the ingenious but computer intensive schemes developed by Kasper et al.[2] The approach essentially treats the F-center like a dye laser, utilizing intracavity CaF_2 galvo plates at near Brewster's angle to tune the optical cavity length continuously. A small voltage dither on the intracavity etalon, in conjunction with phase sensitive detection of the weakly power modulated output, provides sufficient feedback signal to servolock the etalon to the scanning longitudinal mode. This method permits extremely simple manual tuning of the F-center (limited at present to 1.3 cm^{-1} only by the voltage range of the etalon PZT), arbitrarily long concatenated scans, and trivial interfacing to a data acquisition system. The single scan capabilities of the spectrometer are demonstrated (see Fig. 2) on a high resolution spectrum of $Br^*(^2P_{1/2}) \leftarrow Br(^2P_{3/2})$, wherein the hyperfine and isotope structure of the atomic levels has been resolved and analyzed.[1]

B. Herman Wallis Theory for Open Shell Radicals

The OH radical exhibits pronounced curvature in the dipole moment, $\mu(R)$, due to a crossing at small R between states correlating to ionic $[O^-(^2D)$ and $H^+(^1S)]$ and covalent $[O(^3P)+H(^2S)]$ dissociation asymptotes.[3-5] This enormous "electrical anharmonicity," in effect, enhances the higher vibrational overtone transitions ($|\Delta v|>1$) at the expense of diminishing the fundamental transition ($|\Delta v|=1$) strength, and is qualitatively responsible for the extensive near IR wavelength range ($\Delta v = -1, -2, -3 \ldots$) of the atmospheric Meinel band emission. In addition, since $\mu(R)$ exhibits a maximum near the equilibrium separation of OH,

A-1

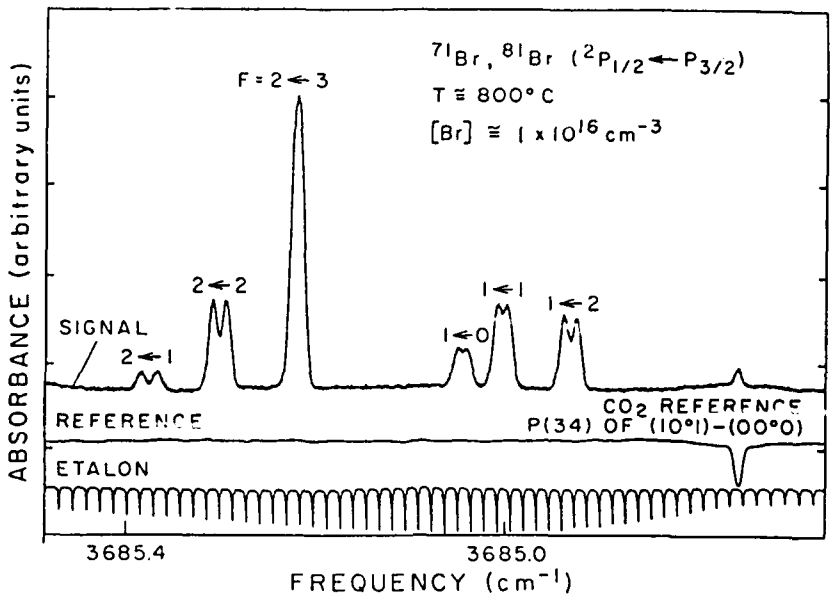

Fig. 2. Single mode continuous scan over the spin orbit transition in atomic bromine, $Br^*(^2P_{1/2}) \leftarrow Br(^2P_{3/2})$.

this curvature is also responsible for large centrifugally induced, end-over-end rotational effects on the $|\Delta v|=1$ fundamental transition moments. These effects, treated in conventional molecules via Herman Wallis theory, are greatly complicated in open shell systems such as $OH(^2\Pi)$ by the coupling of end-over-end ($\underset{\sim}{R}$), orbital ($\underset{\sim}{L}$), and spin ($\underset{\sim}{S}$) angular momenta. In essence, this is because the same total J state can be achieved via several different magnitudes of end-over-end rotation depending on the coupling scheme. Furthermore, in the OH radical this coupling of angular momenta varies between a mixed Hund's case (a and b) at low J to nearly pure Hund's case b at high J, due to the spin angular momentum decoupling from the OH molecular axis for very low values of end-over-end rotation. In order to analyze our data, therefore, we have developed theoretical methods for calculating the IR absorption cross sections for transitions from a specific rotational, vibrational, and spin orbit state for open shell diatomic species. In the case of OH radical,[6,7] the resulting J and ΔJ dependences of these cross sections prove quite dramatic (see Table I), driving specific P, R

branch transitions to nearly zero intensity and casting considerable doubt on previous OH intensity measurements that ignore these rotational effects. Furthermore, we have demonstrated from our calculations that these experimentally observed J and ΔJ dependent relative intensity effects, which rely on concentration independent measurements from a common OH lower state, would permit an accurate inversion of the OH dipole moment function, $\mu(R)$.

C. Flash Kinetic Measurements of OH(v=1←0): Dipole Moment Analysis

As mentioned above in Sec. IIB, our theoretical efforts[6,7] were stimulated by the realization that experimental detection of relative infrared intensities on OH(v,J)←(v',J'), which we accurately measure via flash kinetic spectroscopy, could be utilized to determine the absolute shape of the molecular dipole moment function. Excimer laser photolysis at 193 nm of dilute mixtures of HNO_3 in Ar buffer has been used to prepare well char-acterized OH concentrations in the fast

Table I. Einstein A coefficients[a] (Hz) for selected[b] fundamental/overtone transitions in OH ($X^2\Pi$)

v'←v"	J"	A(Hz) P(J")	Q(J")	R(J")
1←0	0.5	-/-	-/5.6	-/4.4
1←0	1.5	-/12.8	9.6/1.24	3.4/4.6
1←0	2.5	8.4/12.6	3.9/0.61	4.0/4.2
1←0	3.5	10.8/13.1	2.0/0.38	3.8/3.6
1←0	4.5	12.1/13.7	1.2/0.27	3.3/3.0
1←0	5.5	13.2/14.4	0.78/0.21	2.8/2.3
1←0	6.5	14.0/15.0	0.54/0.16	2.2/1.7
2←0	4.5	6.2/6.9	0.81/0.18	3.8/3.9
3←1	4.5	17.7/19.5	2.3/0.52	10.9/11.1
4←2	4.5	33.2/36.6	4.4/0.95	20.4/20.7

[a] Obtained from the dipole moment function, $\mu(R)$, experimentally determined in this work.

[b] The dual entries separated by / refer to transitions from F"=1,2 spin orbit levels, respectively.

flow cell. A tunable F-center laser propagating colinearly with the photolysis pulse then probes the transient OH absorption feature. Laser scans over the line shape profiles are used to obtain the integrated absorption intensities for all rotational and spin orbit transitions with appreciable lower state population at room temperature (see Fig. 3). The IR intensity data plus microwave dipole moments measurements[8] have been analyzed via the methods outlined in Sec. B to determine an experimental OH dipole moment function as a polynomial in $M_n \cdot (R-R_e)^n$, (n=0-3), and which is reliable from R=0.8 Å to 1.2 Å. Interestingly, our dipole moment results (see Fig. 4) compare quite favorably with the ab initio results of both Stevens et al.[3] and Langhoff et al.,[4] but our experimental uncertainties indicate the true $\mu(R)$ lies between the two ab initio curves. With this experimental dipole moment function we can predict the state-to-state infrared cross sections and

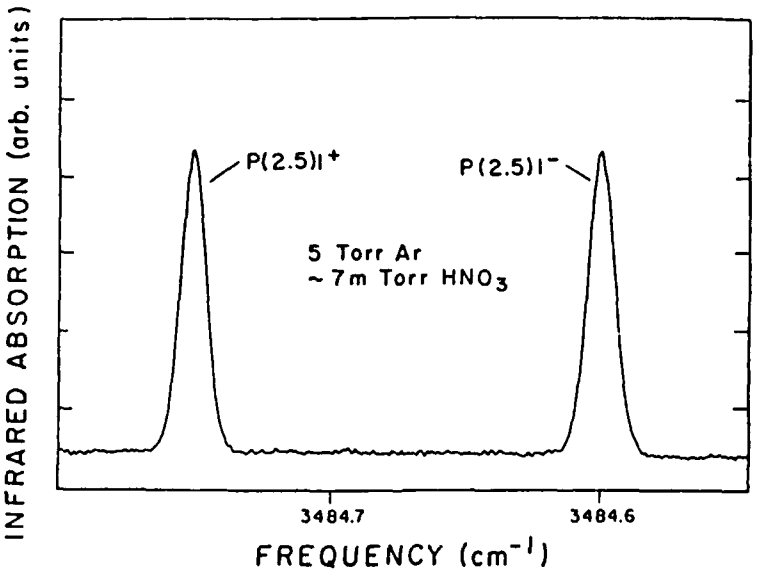

Fig. 3. Sample flash kinetic spectrometer scan over $OH(X^2\Pi)$ Λ-doublets, demonstrating typical signal-to-noise and sensitivity of the instrument.

radiative lifetimes for IR transitions in OH(v,J) for vibrational levels up to $v \lesssim 4$ with an estimated 95% confidence limits of better than 15% (see Table I). By way of comparison, there have been five previous measurements over the past 30 years of the OH($v=1 \leftarrow 0$) transition cross sections,[9-13] with results which have varied by as much as a factor of 5 (see Table II). This serves to underscore the considerable interest, importance and difficulty in measuring this quantity in even such a simple radical system. It is interesting to note the relatively close experimental value of Podolske and Johnston.[12] The Johnston study is based on sensitive diode laser direct absorption in a UV illuminated continuous flow reactor, but relies on an involved kinetic analysis to estimate the absolute steady state concentration of the OH radical.

D. FTIR Emission Studies of $H + O_3 \rightarrow OH(v \leq 9) + O_2$

As a complementary effort to these absorption studies, we have also investigated even higher vibrational levels in OH via rotationally resolved emission data from the $H + O_3$ reaction. These data were obtained via a collaborative effort with C. J. Howard and J. Burkholder at NOAA in Boulder on an existing high resolution Bomem FTIR spectrometer for study of radical reactions. Figure 5 shows sample FTIR data on OH ($\Delta v=-1$) emission from $v \leq 9$ vibrational levels from the chemiluminescent $H + O_3 \rightarrow OH + O_2$ reaction. Data on the overtone emission bands, $\Delta v = -2$ are also obtained and appear as the strongest bands between 4500-7000 cm^{-1}.

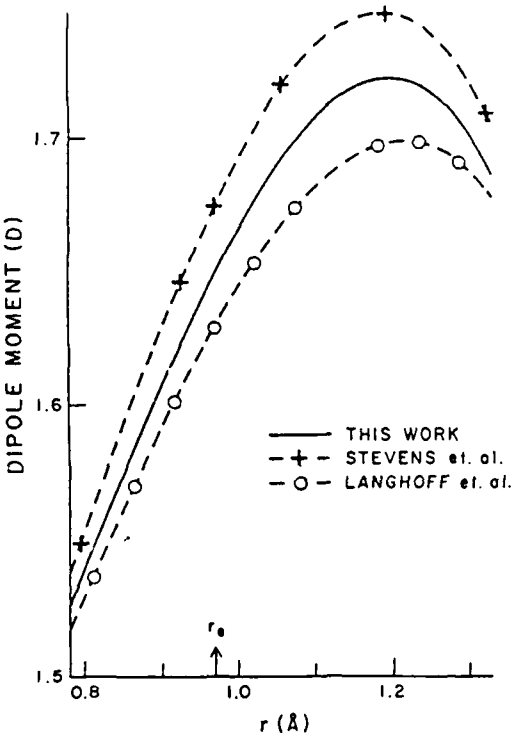

Fig. 4. Empirically determined dipole moment function for OH ($X^2\Pi$), valid between $0.8Å \lesssim R \lesssim 1.2Å$. Also shown are the two best ab initio calculations[3,4] for comparison. Note the expanded dipole moment scale which accentuates the small differences between experiment and theory.

Table II. Previous experimental measurements of rotationless[a] Einstein A coefficients for OH (v=1←0)

Investigators	Year	A (Hz)
Benedict and Plyler (Ref. 9)	1954	33
D'Incan, Efantin and Roux (Ref. 10)	1971	8.5
Roux, D'Incan and Gerny (Ref. 11)	1973	42.5
Podolske and Johnston (Ref. 12)	1983	10.2
Turnbull and Lowe (Ref. 13)	1988	21.
Nelson et al. (Ref. 7)	1988	16.7±1.9[b]

[a] The strong rotational state dependence (Ref. 6) of the radiative lifetimes has been factored out to permit fair comparison of the experimental values.
[b] Uncertainty represents 95% confidence limits.

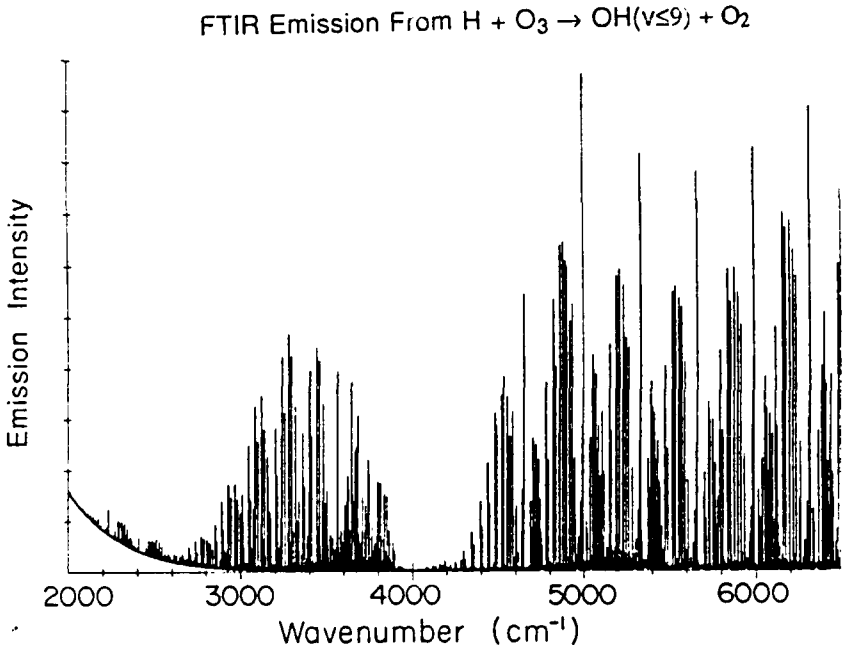

Fig. 5. Sample FTIR emission spectrum from $H + O_3 \rightarrow OH(v \leq 9) + O_2$. The two bands near 3000 cm^{-1} and 5500 cm^{-1} represent fundamental ($\Delta v = -1$) and anomalously strong overtone ($\Delta v = -2$) emission from vibrationally excited states. Baseline curvature at lowest frequencies comes from unstructured blackbody radiation, which is readily corrected for by reference methods.

There are several important issues to address in analyzing data from these emission experiments. First is the fact that OH(v) radicals are cascading radiatively and collisionally to lower levels in the field of view of the spectrometer. Hence the v, J and spin orbit state populations are likely to be far from equilibrium distributions and not at all simple to characterize. We completely circumvent this difficulty by measuring relative emission intensities from a common upper state, and exploit the strong J, ΔJ and spin orbit dependence of the radiative rates to extract the desired dipole moment information. Indeed, it is precisely these centrifugal and angular

momentum effects which made possible our measurements on the $v = 1 \leftarrow 0$ absorption band in a similarly concentration independent fashion.[6,7]

The relative intensities of 88 pairs of rovibrational transitions of OH distributed over 16 vibrational bands have been measured.[14] The data are combined with the previous $v = 1 \leftarrow 0$ absorption data to determine the OH dipole moment function as a cubic polynomial expanded around the equilibrium bond length. The analysis is based on the modified Herman Wallis treatment described above for the pure absorption data. Much larger intermolecular separations are sampled in the higher vibrational levels, and thus the refined dipole moment function now extends from 0.7 to 1.76 Å. Since the key effect on the IR intensities arises from finite vibrational displacement over a highly nonlinear $\mu(R)$, one would predict dramatic differences between the J, ΔJ and spin orbit dependence of OH and OD radiative rates. We are presently testing these predictions via OD(v) emission from the isotopically substituted $D + O_3$ radical reaction as a final confirmation and refinement of the experimentally determined $\mu(R)$.

Our determination of $\mu(R)$ is presently sufficient to permit detailed comparison with ab initio and semi-empirical predictions of transition strengths for the full range of vibrational states (v=0-9) for up to $\Delta v = \pm 3$. Figure 6 demonstrates a particularly illustrative comparison for the first overtone series from $v' = 0, 1, 2, \ldots, 9$. Best agreement with our total experimental measurements are obtained with the theoretical dipole moment function of Langhoff et al.[4] while significant deviations can be noted from predictions based on other theoretical and semi-empirical dipole moment functions in the literature.[3,5,15] Of particular note are the intensities of these overtone transitions, which by virtue of the extreme "electrical

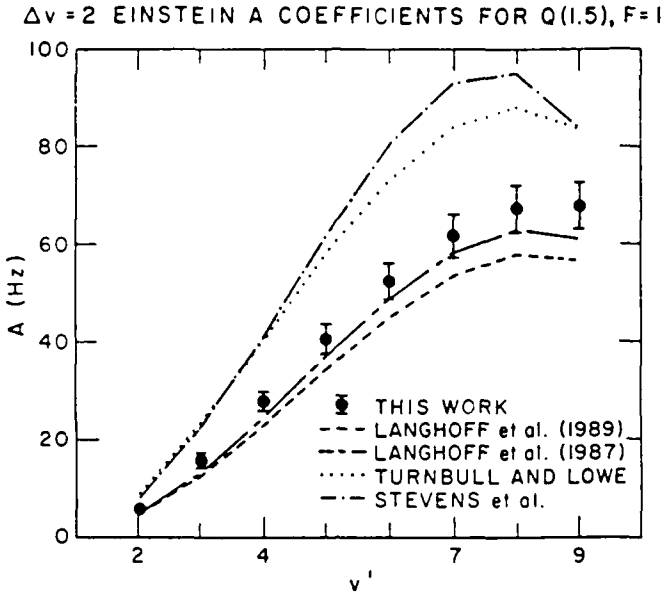

Fig. 6. Δv=2 overtone transition strengths for OH radical in comparison with predictions of ab initio and semi-empirical calculations. Note the extremely strong radiative rates on the overtone transitions for high v due to extreme "electrical anharmonicity" in the dipole moment function. These radiative rates will permit a quantitative IR based laser absorption probe of even the highest vibrational levels of OH.

anharmonicity" of OH, are actually far more intense than the corresponding fundamental transitions for all but lowest vibrational levels. This intensity enhancement can also be readily seen in Table I as well as experimentally in Fig. 5. It is precisely this novel feature of the OH radical that will permit sensitive detection over the entire range of vibrational states of OH via overtone absorption of a tunable 1.5 μm F_2^+ color center laser.

E. Absolute Photolysis Quantum Yields and Pressure Broadening Coefficients

This knowledge of absolute infrared radiative lifetimes can be simply transformed into a measurement of the absolute quantum yields, Φ, for photolytic production of OH. This is demonstrated clearly in Fig. 7, which

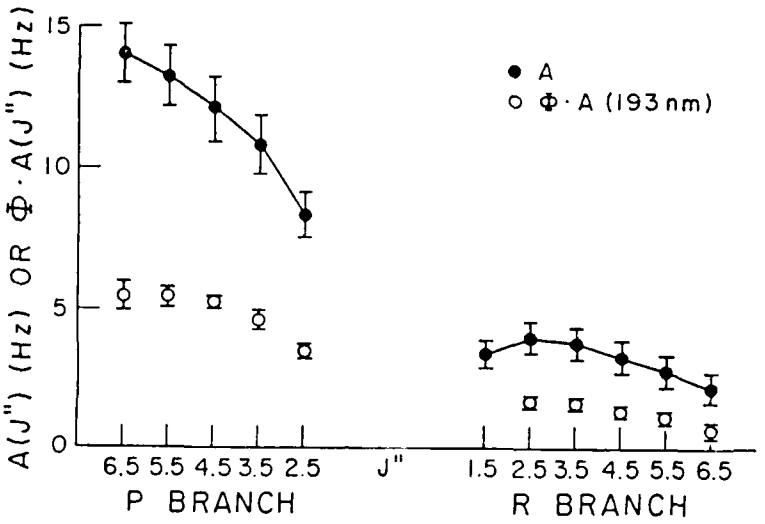

Fig. 7. Radiative rates A, and Φ•A (in Hz) for state-resolved transitions in $OH(^2\Pi)$ (v=1←0) for the F=2 spin orbit state. Φ•A points are measured from absolute direct absorption data for HNO_3 photolysis at 193 nm. The A coefficients are calculated from the $\mu(R)$ determined in this work.

shows a) the Einstein A coefficients for the F=2 spin-orbit state of OH and b) the product of Φ times A (directly obtained from the experiment), plotted against lower state J". The systematically lower values of Φ•A for HNO_3 photolysis at 193 nm implies a quantum yield[16] of only $\Phi_{193} = 0.44 \pm 0.05$. Indeed, since these studies there have been a number of experiments which corroborate the presence of a second photolysis channel[17-19] to form

$$HNO_3 \xrightarrow{193} HONO + O,$$

both by O atom and nitrous acid detection. There have been no previously reported measurements of Φ for HNO_3 photolysis at 193 nm, although measurements by Johnston and coworkers[20] indicate a quantum yield near unity

from 300 nm down to 200 nm. Our measurements,[16] therefore, indicate an unanticipated wavelength dependence to the photolysis branching ratios for HNO_3 in a spectral window relevant in the upper atmosphere (see Table III). This wavelength dependence of Φ may arise from participation of another electronic state, as indeed suggested[21] by the intense UV absorption band at 185 nm.

In order to obtain accurate integrated absorptions, these studies necessitate the measurement of pressure broadening effects in a variety of buffer gases and for a range of rotational, spin orbit, and lambda doublet levels. This has been performed by fitting Voigt line shapes to the data to extract the Lorentzian contribution, $\Delta\nu_L$. Plots of $\Delta\nu_L$ versus buffer gas pressure are then used to extract the desired pressure broadening rates for a specific transition.

A sample plot of pressure broadening of OH(v=1←0) P(2.5) F=1 by N_2 from these studies is shown in Fig. 8. Interestingly, data indicate a general decrease in pressure broadening with increasing J rotational level, due most likely to rapid rotational averaging of the effective potential anisotropy responsible for quantum state changing collisions. A similar trend is observed in closed shell hydrides[22] such as HF. These data suggest a significant collisional metastability of high J rotational states of OH, which

Table III. Absolute photolysis quantum yields, Φ, for OH production.[16]

Species	λ(nm)	Φ
HNO_3	193	0.44±0.05[a]
HNO_3	248	0.63±0.05
H_2O_2	193	1.10±0.10
H_2O_2	248	1.30±0.05

[a] Uncertainty represents 95% confidence limits.

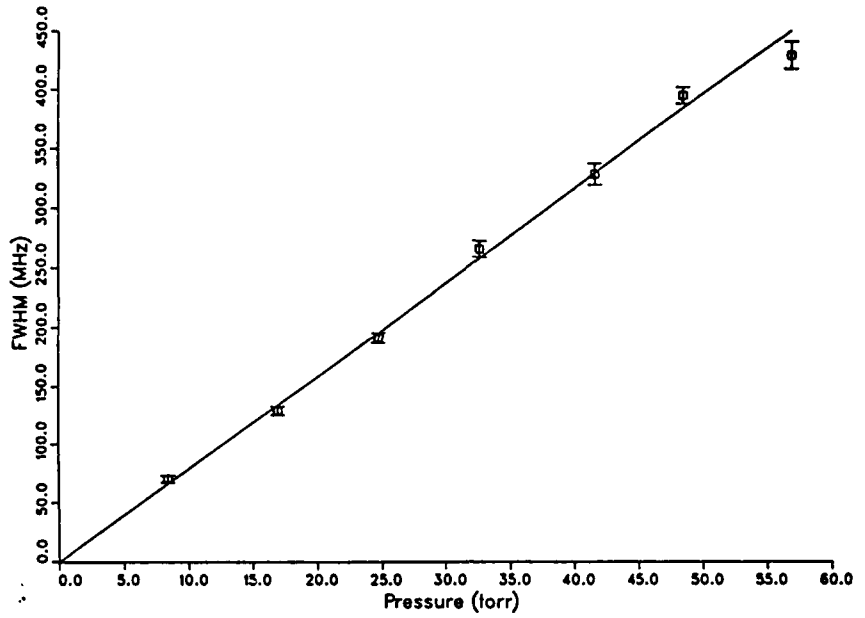

Fig. 8. Pressure broadened linewidths for OH (v=1←0) P(2.5) F=2 as a function of N_2 buffer gas pressure.

would be of considerable relevance to understanding NLTE emission behavior observed in the atmosphere,[23] and which we are proceeding to investigate in real time with the flash kinetic spectrometer.

F. Reactive Kinetics of OH (v=0)

The state-resolved transient absorption signals in the spectrometer are digicized as a function of time and signal averaged. Since the chemical composition of the flow cell can be systematically varied and determined via calibrated flow meters and total cell pressure, this permits fast ($\lesssim$ 1 μsec) kinetics of reactive radicals photolytically formed in the flow cell to be measured in quantitative detail. In addition to its contribution to IR

"airglow" phenomena, the OH radical is one of the most chemically important species in the atmosphere, undergoing reactions such as

$$OH + RH \rightarrow H_2O + R$$

which is an important step in both combustive as well as atmospheric oxidation of hydrocarbons. The flash kinetic IR spectrometer proves to be ideal for study of these OH reactions with excellent band width and signal to noise, and in particular can be readily extended to study of vibrationally enhanced chemistry from OH (v>0). As a demonstration of such kinetic studies, we have investigated the reactions of photolytically formed OH(v=0) with several small hydrocarbons, [RH = ethane, propane, n-butane and isobutane].[24] Figure 9a demonstrates the typical signal to noise of an OH(v=1←0) absorption trace in the presence of n-butane, as well as the excellent single exponential fit over four 1/e lifetimes and residuals for the fit. The observation of the complete OH time dependence is an extremely important advantage to direct, real time measurements, since possible kinetic interferences from chain reactions which regenerate the OH radical become immediately evident. To test for possible systematic errors in the method, we have investigated these reactions over an order of magnitude in OH radical concentrations, and over factors of 50 in reagent pressures, buffer gas identity and pressures, and further confirmed the results on a series of spin orbit, lambda doublet and J rotational transitions. A Stern-Volmer analysis of first order decay rates versus reagent pressures for the series of hydrocarbons is shown in Fig 9b. Rate constants for each of the four reagent gases are summarized in Table IV. Previous measurements[25,26] via a variety of other methods are also shown, indicating the considerable range of values previously obtained. Good agreement is obtained with the recent laser induced fluorescence measurements

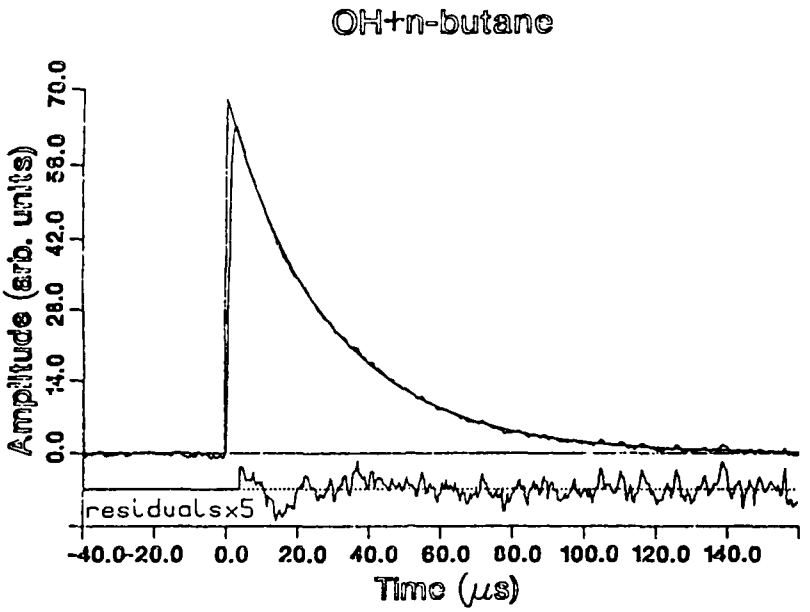

Fig. 9a. Typical flash kinetic absorption signals for OH($X^2\Pi$) P(4.5)$^+$ F-2, v=1←0, in the presence of n-butane. The solid line is a single exponential fit to the data, and residuals are shown below at 5-fold magnification.

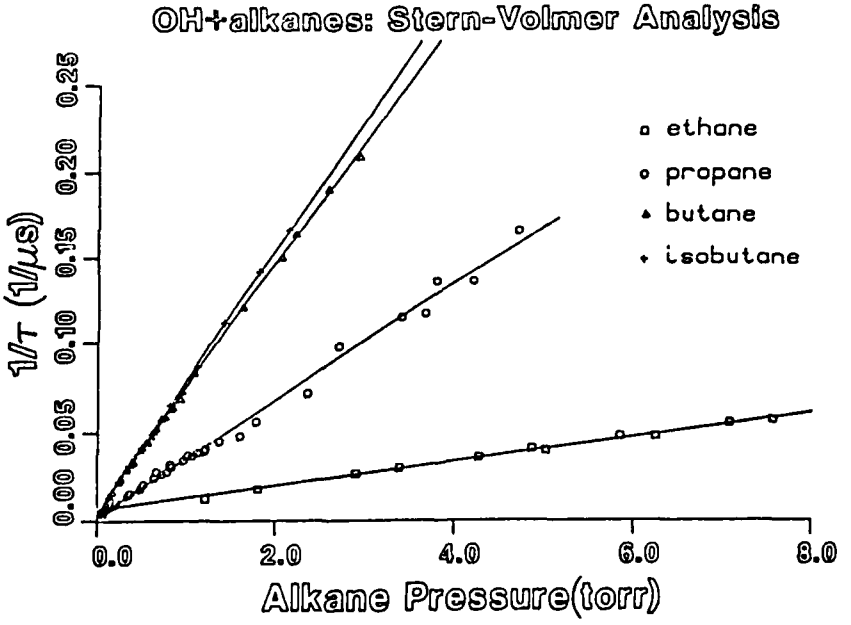

Fig. 9b. Stern-Volmer plots for reaction rates of OH(v=0) with ethane, propane, n-butane and isobutane.

of Tully and coworkers[27] on OH + ethane and propane, which serves as strong confirmation of capability of the spectrometer for quantitative kinetic studies.

Table IV. Rate constants for OH + alkane reactions (units are 10^{-12} cm^3 $molec^{-1}$ sec^{-1}).

reagent	this work	previous results[a)]
ethane	0.243±0.012	0.27±0.04
propane	0.95±0.05	1.10±0.22
butane	2.35±0.08	2.55±0.73
isobutane	2.11±0.09	2.66±0.85

a)± represents the range of values reported from Refs. 25, 26.

References

1. D. D. Nelson Jr., A. Schiffman, K. R. Lykke, and D. J. Nesbitt, Chem. Phys. Lett. **153**, 105 (1988).
2. J. V. V. Kasper, C. R. Pollock, R. F. Curl, and F. K. Tittel, Appl. Opt. **21**, 236 (1982).
3. W. J. Stevens, G. Das, A. C. Wahl, D. Neumann, and M. Krauss, J. Chem. Phys. **61**, 3686 (1974).
4. S. R. Langhoff, H.-J. Werner, and P. Rosmus, J. Mol. Spec. **118**, 507 (1986).
5. H.-J. Werner, P. Rosmus, and E. A. Reinsch, J. Chem. Phys. **79**, 905 (1983).
6. D. D. Nelson, Jr., A. Schiffman, D. J. Nesbitt, and D. J. Yaron, J. Chem. Phys. **90**, 5443 (1989).
7. D. D. Nelson, Jr., A. Schiffman, and D. J. Nesbitt, J. Chem. Phys. **90**, 5455 (1989).

8. K. I. Peterson, G. T. Fraser, and W. Klemperer, Canad. J. Phys. **62**, 1502 (1984).

9. W. S. Benedict and E. K. Plyler, Natl. Bur. Std. Circular, **523**, 57 (1954).

10. J. D'Incan, C. Effantin, and F. Roux, J. Quant. Spectrosc. Rad. Trans. **11**, 1215 (1971).

11. F. Roux, J. D'Incan, and D. Gerny, Astr. J. **186**, 1141 (1973).

12. J. R. Podolske and H. S. Johnston, J. Chem. Phys. **79**, 3633 (1983).

13. D. N. Turnbull and R. P. Lowe, J. Chem. Phys. **89**, 2763 (1988).

14. D. D. Nelson, Jr., A. Schiffman, D. J. Nesbitt, J. J. Orlando, and J. B. Burkholder, J. Chem. Phys. (submitted).

15. D. N. Turnbull and R. P. Lowe, J. Chem. Phys. **89**, 2763 (1988).

16. A. Schiffman, D. D. Nelson, Jr., and D. J. Nesbitt, J. Chem. Phys. (submitted).

17. R. F. Curl (private communication).

18. M. Kozinsky, H. F. Davis III, D. Oh, and Y. T. Lee (private communication).

19. R. D. Kenner, F. Rohrer, Th. Papenbrock, and F. Stuhl, J. Phys. Chem. **90**, 1294 (1986).

20. G. S. Jolly, D. L. Singleton, D. J. McKerney, and G. Paraskevopoulos, J. Chem. Phys. **84**, 6662 (1986); A. R. Ravishankara, F. L. Elsele, and P. H. Wine, J. Phys. Chem. **86**, 1854 (1982); H. S. Johnston, S. Chang, and G. Whitten, J. Phys. Chem. **78**, 1 (1974).

21. H. Johnston and R. Graham, J. Phys. Chem. **77**, 62 (1973).

22. J. P. Sung and D. W. Setser, J. Chem. Phys. **69**, 3868 (1978); D. Raybone, S. J. Wategaonkar, and D. W. Setser, J. Chem. Phys. **89**, 3384 (1988).

24. A. Schiffman, D. D. Nelson, Jr., M. Robinson, and D. J. Nesbitt, J. Chem. Phys. (submitted).

25. W. B. DeMore, M. J. Molina, S. P. Sander, D. M. Golden, R. F. Hampson, M. J. Kurylo, C. J. Howard, and A. R. Ravishankara, Chemical kinetics and photochemical data for use in stratospheric modeling, Jet Propulsion Laboratory Publication 87-41 (1987).

26. D. L. Baulch, M. Bowers, D. G. Malcom, and R. T. Tuckerman, J. Phys. Chem. Ref. Data **15**, 503 (1986).

27. F. P. Tully, A. R. Ravishankara, and K. Carr, Int. J. Chem. Kinet. **15**, 1111 (1983).